Civil Engineering Dimension
https://ced.petra.ac.id

Evaluation of Basal Heave Stability for Deep Excavations in Clay using the Discontinuity Layout Optimization Method

Susiyanti, A.D.M.[1] and Lim, A.[1,2*]
[1] Department of Civil Engineering, Parahyangan Catholic University, Bandung 40141, INDONESIA
[2] Centre of Excellence in Urban Infrastructure Development, Parahyangan Catholic University, Bandung 40141, INDONESIA

DOI: https://doi.org/10.9744/ced.28.1.83-100

Article Info:
Submitted: Jan 20, 2025
Reviewed: Feb 18, 2025
Accepted: Nov 04, 2025

Keywords:
deep excavation,
soft clay,
discontinuity layout optimization method,
basal heave.

Corresponding Author:
Lim, A.
Department of Civil Engineering,
Parahyangan Catholic University,
Bandung 40141, INDONESIA
Email: aswinlim@unpar.ac.id

Abstract

Basal heave is a common failure mechanism in deep excavations in soft clay soils, which often causes significant ground movement and threatens nearby structures. Traditional analysis methods generally assume homogeneous soil conditions and ignore the variation of strength with depth, which limits their application in complex field situations. This research investigates basal heave stability using the Discontinuity Layout Optimization (DLO) method, which identifies critical failure mechanisms by optimizing potential discontinuities in the soil mass. The research examines the influence of undrained shear strength (Su), its gradient, and the excavation width-to-height ratio (B_1 /H) on the safety factor, considering homogeneous and layered soil models. Results show that the safety factor increases with higher Su values but decreases as B_1/H increases. While the DLO method provides reliable predictions for homogeneous soils, but it shows limitations in layered soils. Therefore, for more accurate results in complex stratigraphy, integrating DLO with the Finite Element Method (FEM) is recommended.

INTRODUCTION

Recent studies on deep excavation failures in soft clay have emphasized the potential for excessive soil and wall movements, which may compromise the stability of adjacent structures and underground utilities. Such deformations can occur even in excavations supported by stiff retaining systems, including diaphragm walls, secant pile walls, and multiple strut configurations. In particular, construction-induced ground displacement can result in significant basal heave, further intensifying deformation around the excavation site. This issue is especially critical in coastal regions, where poor geological conditions and thick deposits of soft clay make excavation-related instability more prevalent [1–2]. Consequently, accurately predicting basal heave behavior is essential to preventing deep excavation failures and mitigating the risk of damage to nearby infrastructure.

Conventional approaches for assessing basal heave stability in soft clay excavations—such as those proposed by Terzaghi [3], Bjerrum and Eide [4], and the slip-circle method [5]—are widely used in engineering practice. While these methods have demonstrated practical applicability, they are based on simplifying assumptions, notably that the undrained shear strength of soft clay is homogeneous. Moreover, they often neglect critical factors such as wall stiffness and embedment depth, both of which significantly influence excavation stability. In scenarios where the soft clay beneath the excavation base is sufficiently thick, traditional methods typically assume that the failure surface extends across the entire base, an assumption that may not reflect actual field conditions. Huang et al. [6] highlighted

Note : Discussion is expected before July, 1st 2026, and will be published in the "Civil Engineering Dimension", volume 28, number 2, September 2026.
ISSN : 1410-9530 print / 1979-570X online
Published by : **Petra Christian University**

that the undrained shear strength of soft clay typically increases with depth due to natural sedimentation and consolidation processes. This variation influences the basal heave failure mechanism, often confining the failure surface to deeper soil layers.

Several researchers, including Do et al. [2,7], Faheem et al. [8], Goh [9], and Lim and Ou [10], have investigated the stability of excavations in soft clay using the Finite Element Method (FEM). In a related context, Chen et al. [11] employed rigid finite elements to derive upper-bound solutions for slope stability problems. A distinctive characteristic of FEM-based formulations is that deformation is restricted to occur along predefined element boundaries, as the elements themselves are not capable of deforming freely. This characteristic enables the clear delineation of the critical failure mechanism, which can aid engineers in interpreting failure patterns. However, a major limitation of this approach lies in its sensitivity to mesh topology. The geometry and connectivity of the finite element mesh can significantly influence the predicted failure mechanism, potentially resulting in outcomes that deviate considerably from the actual critical failure mode [12].

As an alternative to traditional methods, Discontinuity Layout Optimization (DLO), introduced by Smith and Gilbert [13], offers a more direct and efficient approach for identifying critical failure mechanisms. Unlike finite element methods, DLO constructs a network of potential discontinuities between discrete points without relying on solid elements. This framework enables the straightforward identification of complex failure patterns and yields results that are more explicit and interpretable for engineering applications. Furthermore, DLO provides enhanced precision in capturing stress and displacement singularities, representing a significant advantage over conventional FEM approaches [12,14].

Although DLO demonstrates significant potential for application across various geotechnical problems, its use in basal heave stability analysis remains relatively limited. Accordingly, this study aims to investigate the applicability of DLO in evaluating basal heave stability in soft clay. To this end, stability analyses were conducted using the *LimitState:GEO* software, which implements the DLO method, under varying soil properties and excavation geometries. Specifically, the study evaluates the influence of undrained shear strength (Su) and the width-to-height ratio (B_1/H) on the factor of safety (SF), while also identifying the limitations of DLO in modeling basal heave conditions in soft clay. Additionally, a comparative analysis with results from the Finite Element Method (FEM) was performed, focusing on both SF values and the predicted failure mechanisms. The findings of this research offer valuable insights into the effectiveness and limitations of DLO for assessing deep excavation stability in soft clay.

METHODS

Basal Heave and Its Mechanism

Basal heave refers to the upward displacement of soil at the base of an excavation, resulting from an imbalance between the overburden pressure exerted by the surrounding soil and the shear strength of the soil within the excavation base. This phenomenon is particularly prevalent in soft clay deposits and poses substantial risks to the stability of deep excavations, potentially leading to structural damage to adjacent infrastructure and disruptions at construction sites. The mechanism of basal heave involves the development of failure surfaces beneath the excavation, which facilitate the upward movement of soil and may ultimately lead to overall excavation failure. A key metric in assessing basal heave stability is the factor of safety (SF), defined as the ratio of the soil's available shear strength to the stresses exerted by the weight of the surrounding soil mass.

Conventional Methods for Basal Heave Analysis

Conventional methods—such as the Terzaghi method [3], Bjerrum and Eide's approach [4], and the slip-circle method [5]—are widely employed to evaluate basal heave stability in soft clay. These techniques generally assume homogeneity in the soil profile and often neglect critical factors such as wall embedment depth and structural stiffness. While practical and straightforward, these methods may fail to accurately capture complex field conditions, particularly in stratified soils or in scenarios where the undrained shear strength increases with depth. A brief overview of these methods is provided below:

- Terzaghi Method: This approach is grounded in classical bearing capacity theory and evaluates basal heave stability by considering soil strength parameters and excavation geometry. It assumes that the failure surface extends across the entire excavation base [3].

- Slip-Circle Method: This method models the failure mechanism as a circular arc and estimates the factor of safety based on soil shear strength and excavation dimensions. While suitable for simple excavation geometries, its accuracy diminishes in layered or heterogeneous soil profiles [5].

Discontinuity Layout Optimization (DLO) Method

The evaluation of geotechnical stability has been the subject of significant methodological advancement. Analytical approaches such as limit equilibrium analyses [4,15–17] and numerical techniques—including the shear strength reduction method applied through the Finite Element Method (FEM) and Finite Difference Method (FDM) [8,18–21]—are commonly employed. Traditional limit equilibrium methods rely on predefined failure surfaces, which can limit their accuracy, particularly in complex geotechnical conditions [22]. Conversely, numerical methods are capable of simulating more intricate soil behaviors but are often computationally demanding and sensitive to mesh discretization.

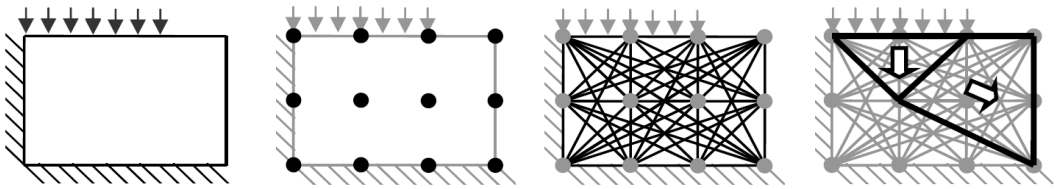

Figure 1. Schematic Diagram of the DLO Working Principle: (a) Initial State, (b) Set the Nodes, (c) Connect the Nodes, (d) Determine the Critical Slip Lines [24]

Discontinuity Layout Optimization (DLO) offers a compelling alternative by enabling limit analysis without the need for predefined failure patterns. This method requires only two fundamental strength parameters—cohesion and the internal friction angle—thus providing a favorable balance between computational efficiency and solution accuracy [23]. Developed by Smith and Gilbert [13], DLO leverages optimization algorithms to directly identify critical failure mechanisms, without depending on complex finite element meshes or assumed failure geometries. As illustrated in Figure 1, the DLO technique discretizes the soil domain into a network of potential discontinuities and uses linear optimization to determine the most critical failure path.

The Discontinuity Layout Optimization (DLO) process involves several key steps:
1. Problem Simplification: Defining the excavation geometry and assigning appropriate soil properties.
2. Discretization: Dividing the soil mass into a network of potential failure lines, consisting of nodes and discontinuities.
3. Optimization: Applying linear optimization techniques to identify the critical subset of discontinuities that collectively form the most likely failure mechanism.
4. Safety Factor Calculation: Determining the factor of safety (SF) based on the identified failure mechanism.

The DLO method is implemented through specialized software such as *LimitState:GEO*, which facilitates the analysis of complex soil conditions and excavation geometries with a high degree of precision. Compared to conventional methods, DLO provides more explicit and interpretable results, offering deeper insight into failure mechanisms—especially in cases involving non-homogeneous soils or spatially varying shear strength gradients.

DLO Modelling

LimitState:GEO software was employed in this study to assess basal heave stability in soft clay using the Discontinuity Layout Optimization (DLO) method. This approach identifies critical failure mechanisms by optimizing potential slip surfaces within the soil domain. The analysis procedure involves defining the excavation geometry, specifying key soil parameters such as undrained shear strength (Su) and total unit weight (γ_t), and computing the factor of safety (SF) to evaluate stability conditions. A series of scenarios were analyzed using a systematic and structured methodology, as outlined below:
1. Geometry setup:
   The excavation geometry was modeled with varying width-to-height ratios (B_1/H) to evaluate the influence of excavation geometry on basal heave stability. The model, implemented in *LimitState:GEO*, is depicted in Figure 2 and was configured as a symmetrical half-space to represent typical excavation conditions. In this setup, the

excavation depth (H) was held constant, while the excavation width (B_1) was systematically varied to simulate both narrow and wide excavations. This approach enables a focused analysis of how variations in the (B_1/H) ratio affect the failure mechanisms and safety factors identified through the DLO method.

2. Soil Properties
   Analyses were conducted under both drained and undrained conditions to reflect realistic soil behavior across various excavation scenarios. Key parameters incorporated into the model included the undrained shear strength (Su), drained cohesion (c′), internal friction angle (ϕ), shear strength gradient (Su gradient), and total unit weight (γt). These properties were varied to evaluate their influence on basal heave stability and to simulate a range of geotechnical conditions representative of soft clay deposits.
3. Application of the DLO Method and Result Interpretation:
   The DLO method was applied to identify the critical failure mechanisms and compute the corresponding factors of safety (SF) for each scenario. The analysis produced clear visualizations of the failure surfaces, offering valuable insights into the influence of different parameters—such as soil strength and excavation geometry—on excavation stability. The results obtained using *LimitState:GEO* were compared with those from the conventional Finite Element Method (FEM) to assess accuracy and consistency. The DLO approach demonstrated high computational efficiency and provided effective visualization of failure mechanisms, particularly in models with homogeneous soil conditions.

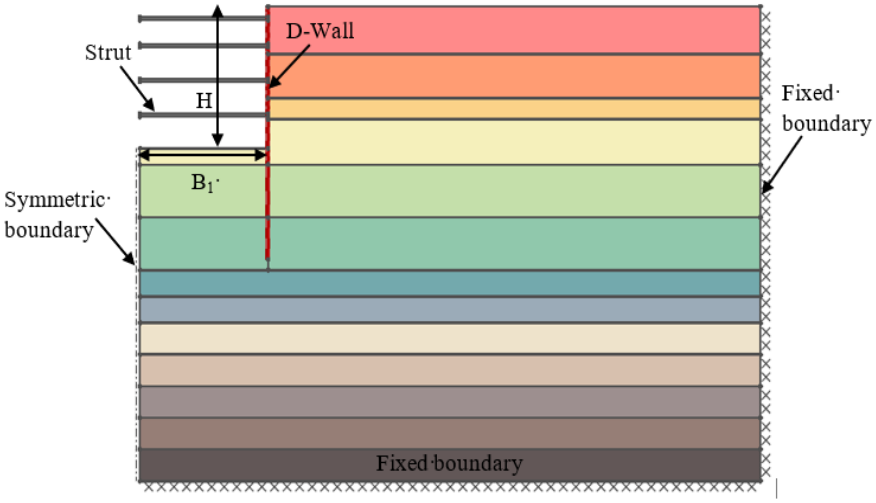

Figure 2. Geometry model of *LimitState:GEO*

RESULTS AND DISCUSSION

This chapter presents the results of a series of analytical scenarios designed to evaluate basal heave stability in deep excavations within soft clay. The analyses were performed using the Discontinuity Layout Optimization (DLO) method implemented in *LimitState:GEO* software. To comprehensively investigate the stability behavior, multiple scenarios were considered by systematically varying key parameters, including the width-to-height ratio (B_1/H), undrained shear strength (Su) and the shear strength gradient. The analyses also accounted for differences in soil stratification, encompassing both homogeneous and layered soil conditions. A summary of the analyzed scenarios, including the varied parameters, number of variations, and specific objectives for each case, is provided in Table 1.
A parametric study was conducted on the width-to-height ratio (B_1/H) to examine the influence of excavation geometry on basal heave stability. The ratio was varied within the range of 0.8 to 1.2 to capture the transition from narrow to medium-width excavations. This range is particularly significant, as even minor changes in geometry can substantially alter the size and shape of the failure mechanism and, consequently, the resulting factor of safety (SF). Prior research by Zheng et al. [25] has shown that the SF tends to decrease with increasing B_1/H before reaching a plateau at a certain threshold, known as the critical width ratio. This threshold distinguishes the geometric regimes between narrow and wide excavations, where further increases in B_1/H no longer significantly affect stability.

In addition to geometric considerations, this study examined the influence of varying soil strength conditions on excavation stability by adjusting the Shear Strength Reduction Ratio (SR). The SR is defined as the ratio of actual shear strength to the reduced shear strength used in the analysis. By systematically varying SR values from 0.8 to 1.2, the study evaluated how changes in soil strength impact the factor of safety (SF) and the corresponding displacement behavior of the soil and retaining structures. This parametric approach provides deeper insight into how

layered soil conditions influence failure mechanisms in deep excavations, particularly in terms of the sensitivity of basal heave stability to strength variability.

Table 1. Scenario of Parametric Study

Case	Parameters	Variations	Number of Variations	Objectives
1	B_1/H	0.5, 0.7, 0.9, 1.0, 1.5, 2.0	6	To analyze the effect of excavation geometry and shear strength reduction (SR) on basal heave stability in layered soil conditions.
	SR	0.8, 0.9, 1.0, 1.1, 1.2	5	
1A	B_1/H	0.5, 0.7, 0.9, 1.0, 1.5, 2.0	6	To analyze the effect of excavation geometry and SR on basal heave stability in homogeneous soil conditions.
	SR	0.8, 0.9, 1.0, 1.1, 1.2	5	
2	B_1/H	0.5, 0.8, 1.0, 1.4, 1.8, 2.0, 2.2, 2.5	8	To analyze the effect of excavation geometry and SR on basal heave stability in layered soil conditions.
	SR	0.8, 0.9, 1.0, 1.1, 1.2	5	
2A	B_1/H	0.5, 0.8, 1.0, 1.4, 1.8, 2.0, 2.5, 5.0	8	To analyze the effect of excavation geometry and undrained shear strength (Su) on basal heave stability in homogeneous soils with a defined Su gradient.
	Initial Su (Su_0)	12.5, 25, 50, 75, 100, 200	6	
	Su gradient	0.25 kPa/m	1	
2B	B_1/H	0.5, 0.8, 1.0, 1.4, 1.8, 2.0, 2.5, 5.0	8	To analyze the effect of excavation geometry and undrained shear strength (Su) on basal heave stability in homogeneous soils without a defined Su gradient.
	Initial Su (Su_0)	12.5, 25, 50, 75, 100, 200	6	
	Su gradient	-	-	
2C	Soil Model	Layered soil (Su: 25 kPa and 50 kPa)	1	To evaluate the influence of large differences in Su between soil layers on failure mechanisms in layered soil models.
	B_1/H	0.5, 0.8, 1.0, 1.4, 1.8, 2.0, 2.5, 5.0	8	
2D	Soil Model	Layered soil (Su: 25 kPa and 30 kPa)	1	To evaluate the influence of small differences in Su between soil layers on failure mechanisms in layered soil models.
	B_1/H	0.5, 0.8, 1.0, 1.4, 1.8, 2.0, 2.5, 5.0	8	

The results are organized according to the predefined scenarios, beginning with layered soil models (Cases 1 and 2), followed by homogeneous soil models (Cases 1A and 2A). These are complemented by specialized analyses addressing the effects of undrained shear strength (Su) gradients (Cases 2A and 2B) and interlayer Su variations (Cases 2C and 2D). The discussion aims to critically evaluate the effectiveness of the DLO method in assessing excavation stability, particularly its capability to capture the geometry and extent of failure mechanisms. The evaluation includes a detailed assessment of the shape and spatial distribution of slip surfaces, with attention to key characteristics such as lateral extent (B′) and rotational depth (R) of the failure zones, both of which are influenced by the underlying soil model and excavation geometry. These observations offer valuable insights into the reliability of the DLO method for identifying critical parameters that govern basal heave stability in both homogeneous and layered soil conditions.

Case 1

Case 1 focused on analyzing the basal heave stability of a rectangular deep excavation situated in Taipei, Taiwan. The excavation measured 100 meters in length and 26 meters in width, as illustrated in Figure 3. The support system consisted of a diaphragm wall (D-wall), 24 meters in length and 0.7 meters in thickness, with a final excavation depth of 13.45 meters. The D-wall was modeled using engineered element properties, incorporating a plastic bending moment capacity (Mp) of 2000 kN·m/m. To simulate wall-soil interaction, a Mohr-Coulomb interface model was applied with a strength reduction factor of 0.7.

Horizontal bracing elements (struts) were represented as rigid members with a unit weight of 78.5 kN/m³, installed at vertical intervals ranging from 4.1 to 5.8 meters. The subsurface profile comprised predominantly silty sand (SM),

silty clay (ML-CL), and soft clay (CL), consistent with typical urban geologies in the region. The groundwater table was located at approximately 2.8 meters below ground level (GL -2.8 m), reflecting common hydrogeological conditions for excavations in Taipei.

The detailed soil parameters (i.e., γ_t, Su, and φ) are presented in **Table 2**. Despite the presence of a diaphragm wall and horizontal bracing system, basal heave failure was observed approximately 2.5 hours after the final excavation depth had been reached. The failure led to the collapse of the internal bracing system and resulted in a significant ground subsidence zone measuring approximately 132 meters in length and 40 meters in width.

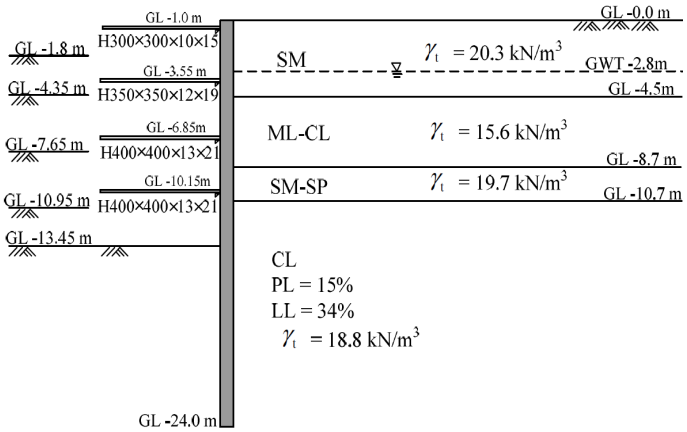

Figure 3. Soil Profile and Construction Stages in Case 1 [26]

Table 2. Mohr-Coulomb Model Soil Parameters for Case 1

Layer	Depth (m)	Soil Type	γ_t (kN/m^3)	N	S_u (kPa)	φ (°)
1	0.0 – 4.5	SM	20.3	14	-	24
2	4.5 – 8.7	ML-CL	15.6	-	15.00	0
3	8.7 – 10.7	SM-SP	19.7	10	-	24
4	10.7 – 15.0	CL	18.8	-	25.00	0
5	15.0 – 20.0	CL	18.8	-	35.00	0
6	20.0 – 25.0	CL	18.8	-	40.00	0
7	25.0 – 27.5	CL	18.8	-	60.50	0
8	27.5 – 30.0	CL	18.8	-	73.70	0
9	30.0 – 33.0	CL	18.8	-	82.56	0
10	33.0 – 36.0	CL	18.8	-	89.84	0
11	36.0 – 39.0	CL	18.8	-	97.12	0
12	39.0 – 42.0	CL	18.8	-	104.40	0
13	42.0 – 45.0	CL	18.8	-	111.68	0

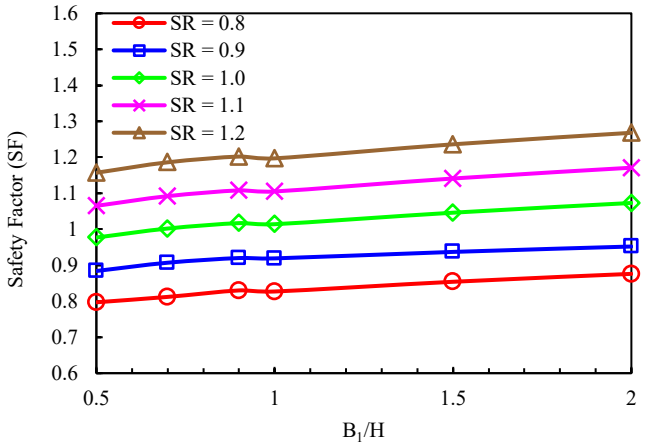

Figure 4. Effect of B_1/H Ratio on SF with Different SR Ratios in Case 1

Figure 4 illustrates the relationship between the excavation width-to-height ratio (B_1/H) and the corresponding factor of safety (SF) for various shear strength reduction ratios (SR). The results indicate a general trend in which SF

increases with B_1/H, suggesting that wider excavations tend to exhibit improved basal heave stability. Additionally, higher SR values—representing stronger soil conditions—correspond to greater SF, underscoring the substantial influence of soil strength on excavation safety. Excavations modeled with lower SR values (e.g., 0.8 and 0.9) show significantly reduced stability, with SF values approaching or falling below the critical threshold of 1.0, indicating potential failure conditions. In contrast, higher SR values (e.g., 1.1 and 1.2) yield noticeably higher SFs, reflecting enhanced stability. While the trend of increasing SF with increasing B_1/H is observed consistently across all SR values, the rate of improvement is relatively moderate, indicating diminishing returns in stability gain as excavation width continues to increase. These findings highlight the critical interplay between excavation geometry and soil strength in ensuring excavation safety. In particular, they emphasize the importance of maintaining an adequate SR to achieve a robust and stable design.

Figure 5 illustrates the basal heave failure mechanisms for Case 1 under an SR value of 1.0, comparing different width-to-height ratios (B_1/H). The results demonstrate a significant evolution in the extent and geometry of failure surfaces as B_1/H increases.

At B_1/H=0.5 (Figure 5a), the failure mechanism is relatively localized, with slip surfaces confined near the excavation base, indicating a restricted instability zone. At B_1/H =1.0 (Figure 5b), the failure surfaces extend further into the surrounding soil, suggesting increased deformation and a broader influence of basal heave. When B_1/H =2.0 (Figure 5c), the failure mechanism becomes significantly more extensive, characterized by deeper and wider slip surfaces that reflect a more pronounced basal heave effect.

This trend indicates that as excavation width increases, the mobilized soil mass also expands, influencing both deformation behavior and the resulting factor of safety (SF). These findings emphasize the critical role of excavation geometry in stability assessments and the importance of design considerations to mitigate basal heave failure. Additionally, the lateral extent of the failure mechanism (B′)—defined as the intersection of the slip surface with the ground surface—increased with larger B_1/H values, growing from 21.4 meters at B_1/H = 0.5 to 23.5 meters at B_1/H=2.0. In contrast, the rotational depth (R) remained nearly constant at approximately 14.7 meters, suggesting that the depth of the failure surface did not significantly extend with increasing width. This indicates that while the lateral spread of instability increases with excavation width, the depth of failure remains largely confined to the weaker, soft clay layers.

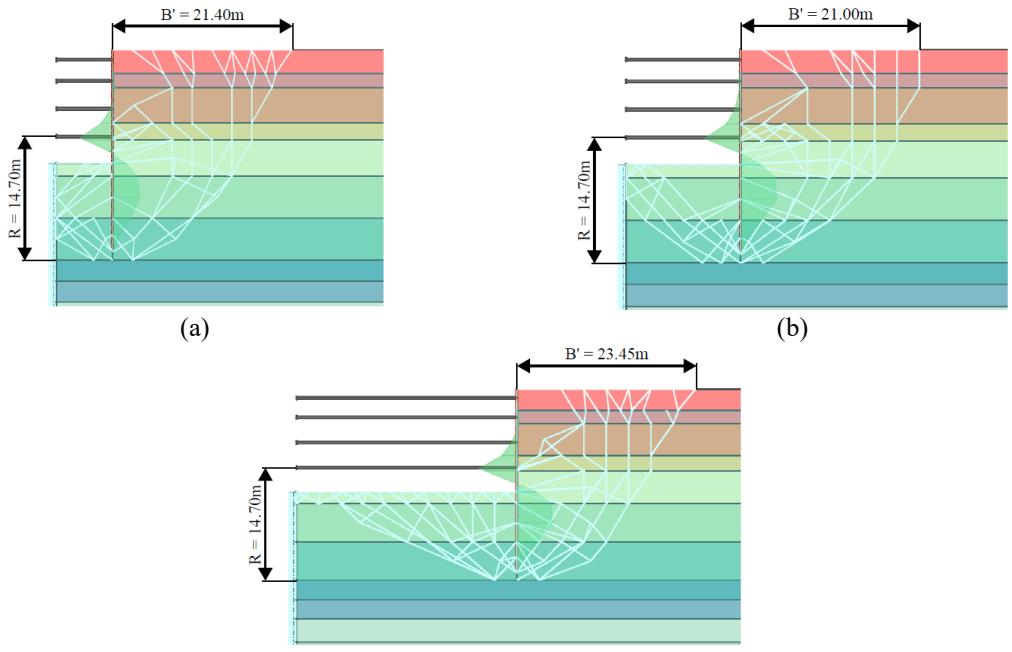

Figure 5. Basal Heave Failure Mechanisms in Case 1 (SR = 1): (a) B_1/H = 0.5 (b) B_1/H = 1.0 (c) B_1/H = 2.0

Case 1A employed the same excavation geometry as Case 1 but simplified the soil stratigraphy by replacing the clay layers between depths of 10.7 m and 45.0 m with a single, homogeneous clay layer. This layer was characterized by a depth-dependent undrained shear strength (Su) gradient of 0.27 kPa/m. The initial undrained shear strength at the top of the clay layer (Su_0) was set to 37 kPa, as summarized in Table 3. The variation of Su with depth was defined by the linear relationship:

$$S_u = S_{u0} + 0.27z$$

where z represents the depth in meters. This formulation allows for a more realistic representation of strength gain with depth due to consolidation, while still maintaining a simplified soil model for comparative analysis.

The results, presented in Figure 6, demonstrate that the factor of safety (SF) decreases with increasing width-to-height ratio (B_1/H), consistent with theoretical expectations for basal heave stability. Under an SR value of 1.0, the SF decreased from 1.15 at B_1/H=0.5 to 0.98 at B_1/H=2.0, indicating reduced stability with wider excavations. Conversely, higher SR values were associated with increased SF across all B_1/H scenarios. For example, at SR = 1.2, the SF rose from 1.13 at B_1/H =0.5 to 1.29 at B_1/H=2.0, highlighting the stabilizing effect of enhanced soil strength. These findings underscore the significance of incorporating a realistic undrained shear strength gradient (Su) in stability analyses. The presence of a depth-dependent Su profile contributes to increased resistance against basal heave, particularly in deeper soil layers, thereby improving overall excavation stability.

Table 3. Mohr-Coulomb Model Soil Parameters for Case 1A

Layer	Depth (m)	Soil Type	γ_t (kN/m^3)	N	S_u (kPa)	φ (°)
1	0 – 4.5	SM	20.3	14	-	30
2	4.5 – 8.7	ML-CL	15.6	-	28.65	0
3	8.7 – 10.7	SM-SP	19.7	10	-	30
4	10.7 – 45.0	CL	18.8	-	37.00	0

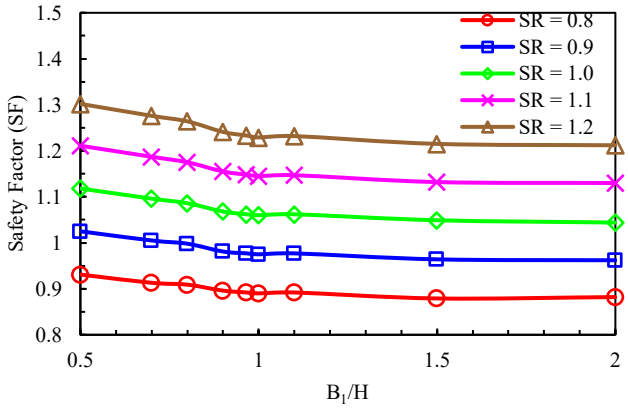

Figure 6. Effect of B_1/H Ratio on SF with Different SR Ratios in Case 1A

The failure surfaces observed in Case 1A exhibited more realistic and continuous behavior compared to those in Case 1, due to the homogeneous soil model incorporating a depth-dependent Su gradient. As illustrated in Figure 7, the lateral extent of the failure mechanism (B′) expanded significantly with increasing B_1/H, ranging from 47.0 meters at B_1/H=0.5 to 63.9 meters at B_1/H=2.0. Likewise, the rotational depth (R) increased from 28.4 meters to 50.6 meters over the same range, indicating a deeper and more extensive failure mechanism within the homogeneous clay layer. This behavior stands in contrast to Case 1, where the presence of stratified soil layers constrained the depth and spread of failure, limiting both B′ and R. The results from Case 1A suggest that the continuous increase in shear strength with depth allows for the development of larger failure zones, thereby offering clearer insights into the influence of soil strength distribution on basal heave mechanisms.

The Discontinuity Layout Optimization (DLO) method demonstrated superior performance in Case 1A, effectively capturing a broader and more realistic failure mechanism under homogeneous soil conditions. The observed expansion of both the lateral extent (B′) and rotational depth (R) reflects the failure zone's sensitivity to excavation geometry and the depth-dependent variation in soil strength. These results are consistent with findings by Lim and Ou [10] and Faheem et al. [8], who also reported a decreasing factor of safety (SF) with increasing B_1/H ratios in homogeneous clay. This trend can be attributed to the progressive increase in undrained shear strength (Su) with depth, which enhances the stability of deeper soil layers and suppresses the formation of shallow basal heave failure zones. Furthermore, Zheng et al. [25] observed that in layered soil profiles, sliding surfaces tend to develop downward, leading to localized failures beneath the excavation base rather than fully mobilized failure mechanisms. This highlights a key limitation of the DLO method in layered soils, where it may underestimate the stabilizing influence of stiffer bottom layers. In contrast, the Finite Element Method (FEM) has proven more effective in

modeling progressive failure and strength mobilization in stratified soils, as demonstrated in studies by Chen et al. [1] and Do et al. [2]. These findings underscore the importance of selecting an appropriate analytical method based on soil heterogeneity and the complexity of the failure mechanism being investigated.

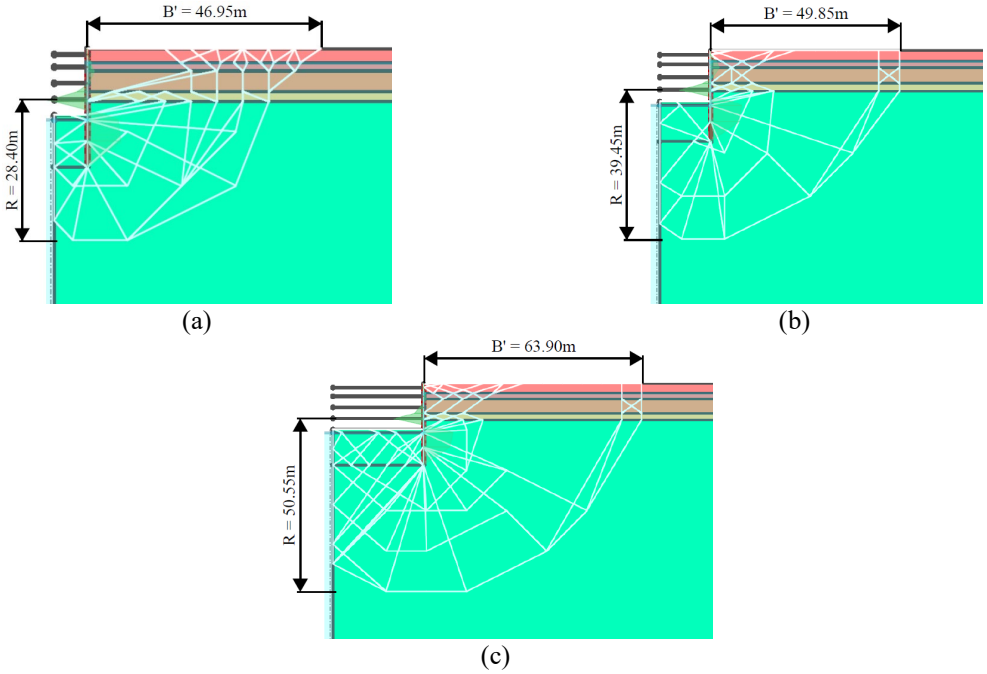

Figure 7. Basal Heave Failure Mechanisms in Case 1A (SR = 1): (a) $B_1/H = 0.5$ (b) $B_1/H = 1.0$ (c) $B_1/H = 2.0$

Case 2

Case 2 involved the analysis of a rectangular excavation site located in Taipei, Taiwan, measuring 12.3 meters in length and 45 meters in width. The excavation was supported by a diaphragm wall (D-wall) with lengths varying between 13.8 meters and 17.0 meters, with an average length of 15.4 meters and a wall thickness of 0.5 meters. The D-wall was modeled using engineered element properties, incorporating a plastic bending moment capacity (Mp) of 2000 kN·m/m. To simulate wall-soil interaction, a Mohr-Coulomb interface model was applied with a strength reduction factor of 0.7.

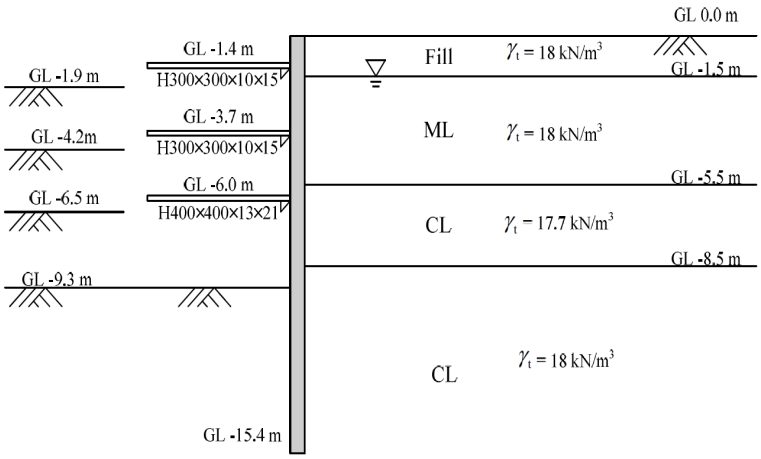

Figure 8. Soil Profile and Construction Stage in Case 2 [26]

The horizontal bracing system (struts) was modeled as rigid elements with a unit weight of 78.5 kN/m³, and was installed to provide lateral support throughout the excavation process. The final excavation depth reached 9.3 meters. This case configuration aimed to assess the basal heave stability in a broader excavation setting, incorporating realistic structural support and soil-structure interaction parameters.

The subsoil profile for Case 2, as illustrated in Figure 8 and detailed in Table 4, consisted of a fill layer overlying a thick silty clay (CL) deposit. The undrained shear strength (Su) of the silty clay increased with depth, ranging from 4.05 kPa near the surface to 81.26 kPa in the deeper layers. The groundwater table was positioned at approximately GL -1.5 meters, contributing to elevated pore pressure conditions during excavation. Despite the implementation of a diaphragm wall and a horizontal bracing system, basal heave failure occurred shortly after the final excavation depth was reached, resulting in significant ground deformation and the eventual collapse of the excavation support structure.

Table 4. Mohr-Coulomb Model Soil Parameters for Case 2

Layer	Depth (m)	Soil Type	γ_t (kN/m^3)	S_u (kPa)	φ (°)
1	0 – 1.5	FILL	18.0	4.05	0
2	1.5 – 5.5	ML	18.0	13.00	0
3	5.5 – 8.5	CL	17.7	17.00	0
4	8.5 – 11.5	CL	18.0	20.73	0
5	11.5 – 14.5	CL	18.0	26.35	0
6	14.5 – 17.5	CL	18.0	34.00	0
7	17.5 – 20.5	CL	18.0	40.91	0
8	20.5 – 23.5	CL	18.0	46.17	0
9	23.5 – 26.5	CL	18.0	52.02	0
10	26.5 – 29.5	CL	18.0	57.87	0
11	29.5 – 32.5	CL	18.0	63.71	0
12	32.5 – 35.5	CL	18.0	69.56	0
13	35.5 – 38.5	CL	18.0	75.41	0
14	38.5 – 41.0	CL	18.0	81.26	0

The failure mechanisms observed in Case 2 were notably more complex than those in Case 1, primarily due to the influence of layered soil conditions. Slip surfaces tended to propagate horizontally along the weaker silty clay strata, which provided reduced resistance to uplift, thereby facilitating basal heave. As shown in Figure 9, the factor of safety (SF) exhibited a slight increase with increasing B_1/H, contrary to the typical expectation that wider excavations reduce stability. For instance, at an SR value of 1.0, SF increased from 0.85 at B_1/H=0.5 to 1.05 at B_1/H=2.5. This deviation is likely attributable to the interaction between excavation geometry and the distribution of strength within the layered soil, where wider excavations may engage deeper, stronger layers, thereby improving overall stability.

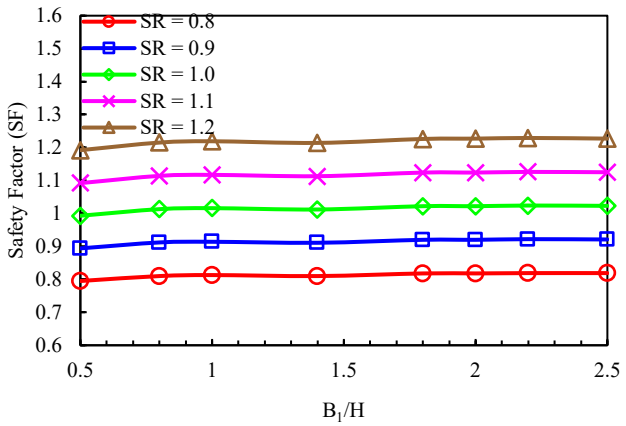

Figure 9. Effect of B_1/H Ratio on SF with Different SR Ratios in Case 2

Additionally, the failure surfaces depicted in Figure 10 reveal that narrower excavations exhibited broader and more extensive failure zones, highlighting a key limitation of *LimitState:GEO* when modeling layered soil conditions. In these cases, the software may not fully capture the complex interaction between weak and strong soil layers, leading to potentially conservative or oversimplified representations of failure mechanisms.

The lateral extent (B′) and rotational depth (R) of the failure surfaces in Case 2 provided further insight into this behavior. At lower B_1/H ratios—corresponding to narrower excavations—both B′ and R were relatively large, indicating more widespread failure zones in both horizontal and vertical directions. For example, at B_1/H=0.5, B reached 16.2 meters and R extended to 11.45 meters. In contrast, at B_1/H=2.5, B′ decreased to 8.15 meters, and R reduced to 9.4 meters. This inverse relationship suggests that narrower excavations are more susceptible to deeper

and wider basal heave failure mechanisms in layered soil, which may not be fully addressed by DLO-based tools like *LimitState:GEO* without more advanced modeling of soil stratigraphy.

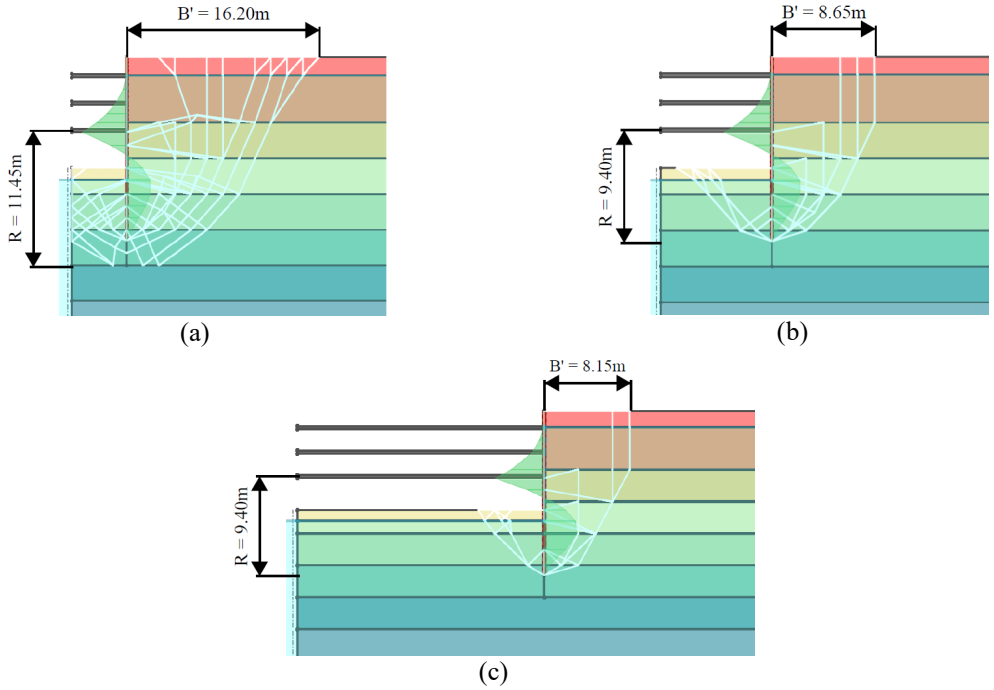

Figure 10. Basal Heave Failure Mechanisms in Case 2 (SR = 1): (a) $B_1/H = 0.5$ (b) $B_1/H = 1.0$ (c) $B_1/H = 2.5$

In Case 2A, the excavation geometry remained identical to that of Case 2; however, the soil profile was simplified into a homogeneous clay layer incorporating a depth-dependent undrained shear strength gradient. The initial undrained shear strength (Su_0) was varied across six values—12.5, 25, 50, 75, 100, and 200 kPa—combined with a linear gradient of 0.25 kPa/m. These values were derived from the stratified profile in Case 2 to evaluate how increasing shear strength with depth influences basal heave stability. The details of the parameter set are summarized in Table 4. Conversely, in Case 2B, the soil was also modeled as homogeneous but with a constant undrained shear strength throughout the depth, eliminating the influence of a strength gradient. This configuration enabled a direct comparison between gradient and non-gradient conditions, isolating the effect of the shear strength gradient on the factor of safety and failure mechanism development.

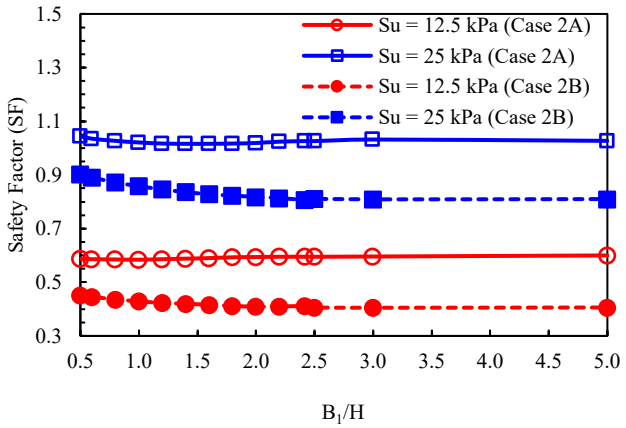

Figure 11. Effect of B_1/H Ratio on SF with Different SR Ratios in Case 2A & 2B (Su = 12.5 & 25 kPa)

The results for Cases 2A, 2B, 2C, and 2D are presented in Figures 11, 12, and 13. In Case 2A, where a positive undrained shear strength (Su) gradient was applied, the factor of safety (SF) consistently decreased with increasing B_1/H, reflecting the influence of excavation geometry on basal heave stability. For example, at Su=12.5 kPa (Figure 11), SF declined from 1.10 at B_1/H=0.5 to 0.90 at B_1/H=5.0. Similarly, at a much higher Su=200 kPa (Figure 13), SF decreased from 7.4 to 6.5 over the same range. These results demonstrate that, despite higher initial strength, wider excavations are more susceptible to basal heave due to broader mobilization of soil mass. The lateral extent (B′) and rotational depth (R) in Case 2A further underscored the stabilizing effect of the Su gradient. For instance, at Su=50

kPa and B_1/H=5.0, B′ reached 49.87 meters and R extended to 40.42 meters, indicating deeper and broader failure mechanisms enabled by increasing the strength with depth.

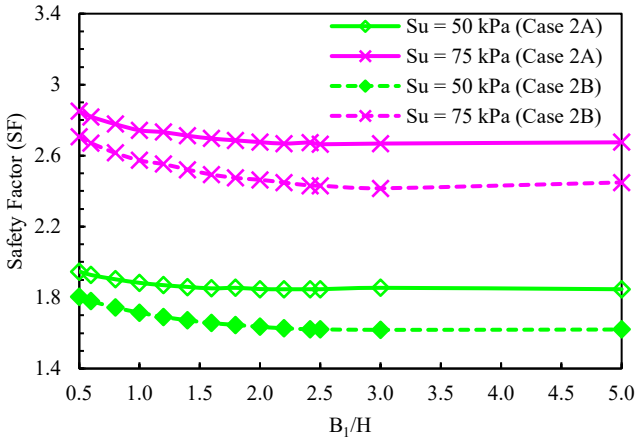

Figure 12. Effect of B_1/H Ratio on SF with Different SR Ratio in Case 2A & 2B (Su = 50 & 75 kPa)

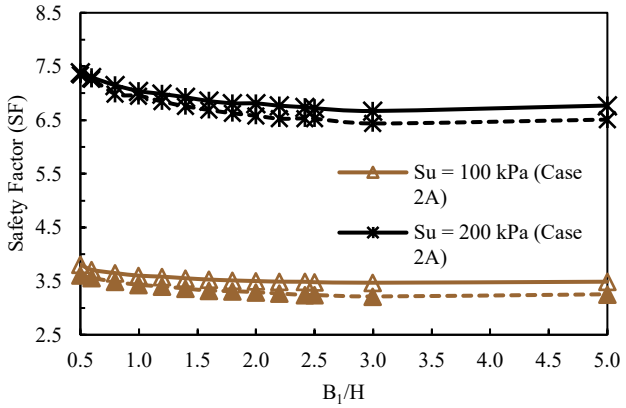

Figure 13. Effect of B_1/H Ratio on SF with Different SR Ratios in Case 2A & 2B (Su = 100 & 200 kPa)

In contrast, Case 2B, which assumed a constant Su with depth (i.e., no gradient), yielded lower SF values for equivalent initial strengths. The absence of a strength gradient limited the ability of deeper layers to resist failure, leading to more constrained failure zones. At Su=50 kPa and B_1/H=5.0, for example, B′ was 49.29 meters and R was 43.4 meters—values slightly smaller and less efficient in mobilizing resistance compared to Case 2A. This comparison reinforces the importance of incorporating realistic Su gradients in excavation design, as they allow deeper layers to contribute more effectively to overall stability.

Cases 2C and 2D introduced stratified soil models to evaluate the effect of distinct layered properties on failure mechanisms. In Case 2C, the upper layer was assigned Su of 25 kPa and the lower layer, Su of 50 kPa, as summarized in Table 5, simulating a scenario with pronounced strength contrasts between layers.

Table 5. Mohr-Coulomb Model Soil Parameters for Case 2C

Layer	Depth (m)	Soil Type	γ_t (kN/m^3)	S_u (kPa)	φ (°)
1	0 – 25	CL	18	25	0
2	25 – 50	CL	18	50	0

In contrast, Case 2D modeled a more gradual transition in undrained shear strength, assigning an Su of 25 kPa to the upper layer and 30 kPa to the lower layer, as detailed in Table 6. This configuration was designed to simulate subsurface conditions with minimal contrast between soil layers, thereby enabling an evaluation of how relatively small differences in strength influence basal heave stability. By comparing Cases 2C and 2D, the study aimed to assess the sensitivity of failure mechanisms to interlayer strength variation and to determine the extent to which even subtle stratification can affect the size, shape, and depth of the failure zone.

Table 6. Mohr-Coulomb Model Soil Parameters for Case 2D

Layer	Depth (m)	Soil Type	γ_t (kN/m^3)	S_u (kPa)	φ (°)
1	0 – 25	CL	18	25	0
2	25 – 50	CL	18	30	0

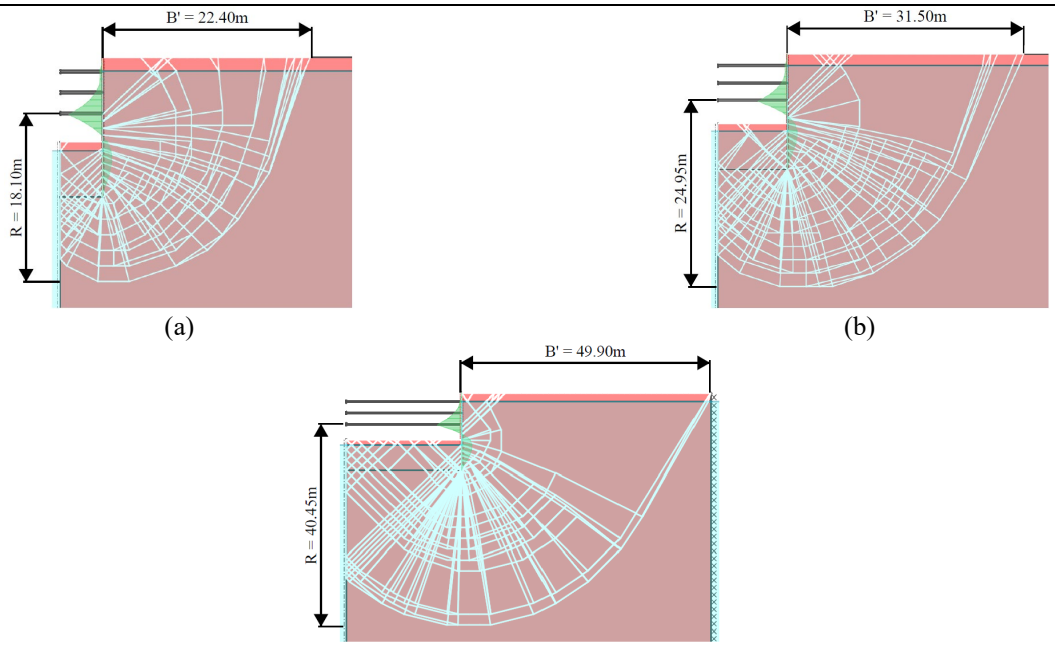

Figure 14. Basal Heave Failure Mechanisms in Case 2A (Su_0 = 50 kPa): **(a)** B_1/H = 0.5 **(b)** B_1/H = 1.0 **(c)** B_1/H = 5.0

Figure 14 illustrates the basal heave failure mechanisms for Case 2A at an initial undrained shear strength (Su_0) of 50 kPa, across varying width-to-height ratios (B_1/H). The failure patterns exhibit distinct changes in extent and geometry as B_1/H increases. At B_1/H=0.5 (Figure 14a), the failure surface is relatively shallow and concentrated near the excavation base, indicating a localized and confined instability zone. When B_1/H=1.0 (Figure 14b), the slip surface broadens, extending further into the surrounding soil and suggesting a higher degree of mobilized deformation. At B_1/H=5.0 (Figure 14c), the failure mechanism becomes significantly more extensive, with deep-seated slip surfaces propagating well beyond the excavation limits, reflecting widespread mobilization of the soil mass.

This progression demonstrates that increasing excavation width leads to more expansive and deeper failure mechanisms, which in turn impact the factor of safety (SF) and deformation behavior. These findings highlight the importance of considering both excavation geometry and depth-dependent soil strength in basal heave stability assessments. Failure to do so may underestimate potential failure extents and associated risks, particularly in deep or wide excavations within soft clay deposits.

Figure 15 presents the basal heave failure mechanisms for Case 2B at an initial undrained shear strength (Su_0) of 50 kPa, considering varying width-to-height ratios (B_1/H). As B_1/H increases, the failure surfaces expand, indicating more extensive mobilization of soil mass. At B_1/H=0.5 (Figure 15a), the failure mechanism remains relatively shallow and localized near the base of the excavation, suggesting a confined instability zone. At B_1/H=1.0 (Figure 15b), the failure surface deepens and broadens, reflecting increased deformation and soil mobilization. At B_1/H =5.0 (Figure 15c), a significantly larger and deeper failure mechanism is observed, encompassing a wide region around and beneath the excavation. Compared to Case 2A, the failure surfaces in Case 2B appear more curved and exhibit more pronounced deep-seated behavior. This suggests that the absence of a shear strength gradient in Case 2B results in a fundamentally different failure pattern, emphasizing the sensitivity of failure mechanisms to soil strength assumptions. These results reinforce the importance of incorporating realistic soil strength profiles—such as depth-dependent Su gradients—when evaluating excavation stability. Figures 14 and 15, when analyzed in tandem, highlight how increasing B_1/H from 0.5 to 5.0 leads to progressively larger and deeper failure zones in both homogeneous conditions with and without Su gradients. However, the failure mechanisms in Case 2B demonstrate a more curved and deeper-seated geometry, indicating that even subtle differences in soil modeling assumptions can significantly affect predicted failure behavior. These findings underscore the critical role of accurate soil characterization and excavation geometry in the reliable assessment of basal heave stability in deep excavations.

As shown in Figure 16, the factor of safety (SF) initially decreased as width-to-height ratio (B_1/H) increased, but eventually stabilized—or slightly increased—at higher values. In Case 2C, SF ranged from 0.85 at B_1/H =0.5 to 0.90 at B_1/H =3.0. A similar trend was observed in Case 2D, where SF stabilized around 0.90 for B_1/H values greater than 3.0, suggesting a limit beyond which further increases in excavation width had minimal effect on overall stability. The failure mechanisms in these cases, depicted in Figures 17 and 18, reveal the influence of soil stratification on the extent (B′) and depth (R) of failure surfaces. In Case 2C, the lateral extent B′ remained relatively small, and the rotational depth R was confined to the weaker upper soil layer. This behavior indicates that failure was predominantly governed by the strength limitations of the top stratum, with limited mobilization of the more competent lower layer. In contrast, Case 2D, which featured a more gradual strength transition between layers, exhibited more extensive failure surfaces as excavation width increased. At B_1/H =5.0, the lateral extent B′ reached 99.25 meters, compared to only 23.1 meters in Case 2C. The deeper and wider failure mechanism in Case 2D allowed greater engagement of the stronger lower layer, thereby contributing to the stabilization of SF at higher excavation widths.

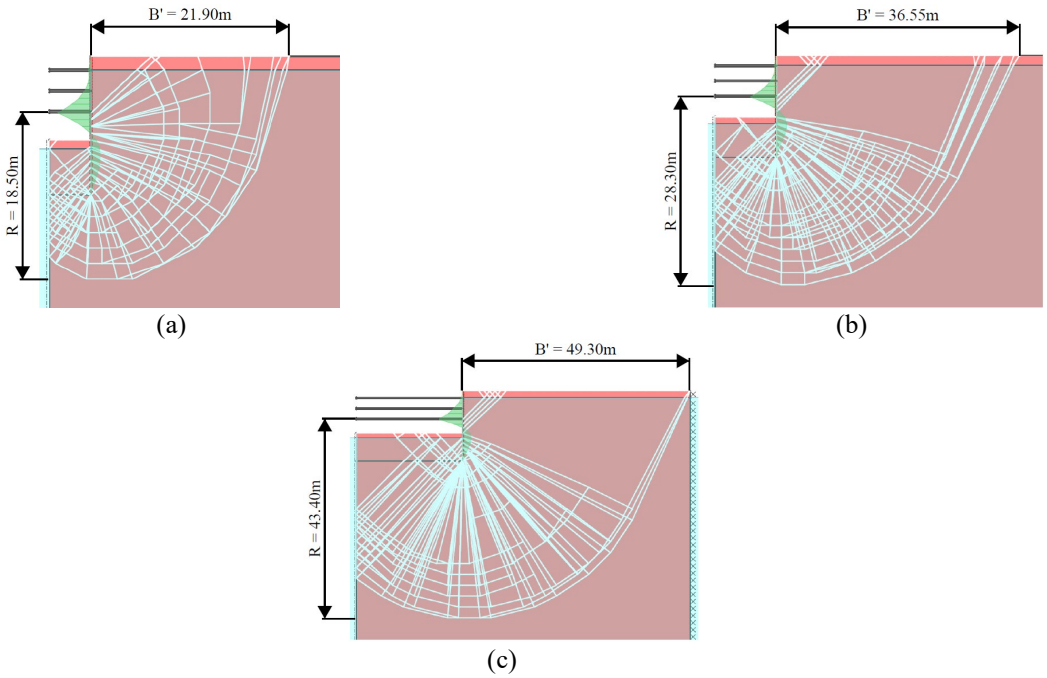

Figure 15. Basal Heave Failure Mechanisms in Case 2B (Su_0 = 50 kPa): (a) B_1/H = 0.5 (b) B_1/H = 1.0 (c) B_1/H = 5.0

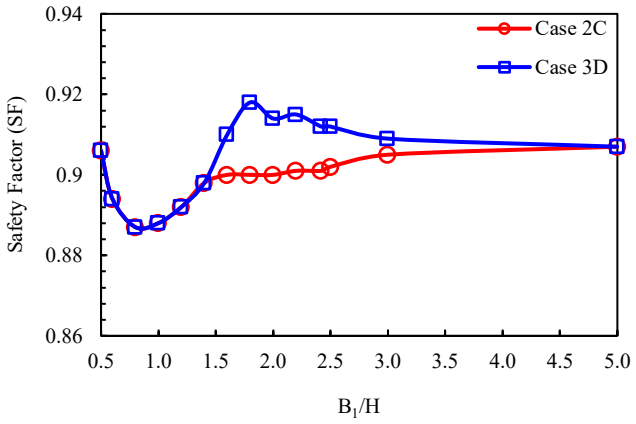

Figure 16. Effect of B_1/H Ratio on SF in Case 2C & 2D

The findings from Cases 2, 2A, 2B, 2C, and 2D underscore the pivotal influence of soil properties—particularly the undrained shear strength (Su) and its gradient—on basal heave stability in deep excavations. The lateral extent (B′) and rotational depth (R) of failure surfaces provided key indicators of the failure zone's reach and depth under varying geotechnical conditions. In homogeneous soil models (Cases 2A and 2B), higher shear strength reduction ratios (SR) and steeper Su gradients led to enhanced stability by expanding both B′ and R, effectively distributing deformation across a broader zone and mitigating localized failure. In stratified soil conditions (Cases 2, 2C, and 2D), failure mechanisms were largely governed by the weaker upper layers, while stronger underlying strata played a critical role

in resisting deeper failure and stabilizing the factor of safety at higher B_1/H ratios. Notably, more gradual interlayer strength transitions, as modeled in Case 2D, allowed for more extensive mobilization of stronger layers, resulting in deeper and more stable failure mechanisms compared to sharply stratified profiles. These results highlight the necessity of accurately characterizing and modeling soil strength distributions—particularly in layered systems—to reliably predict critical failure mechanisms and ensure safe excavation designs. While the Discontinuity Layout Optimization (DLO) method proved effective in identifying potential failure patterns and quantifying SF in homogeneous soils, its limitations in handling complex stratigraphy suggest the need for complementary techniques, such as the Finite Element Method (FEM), for more nuanced and reliable stability analyses in layered ground conditions.

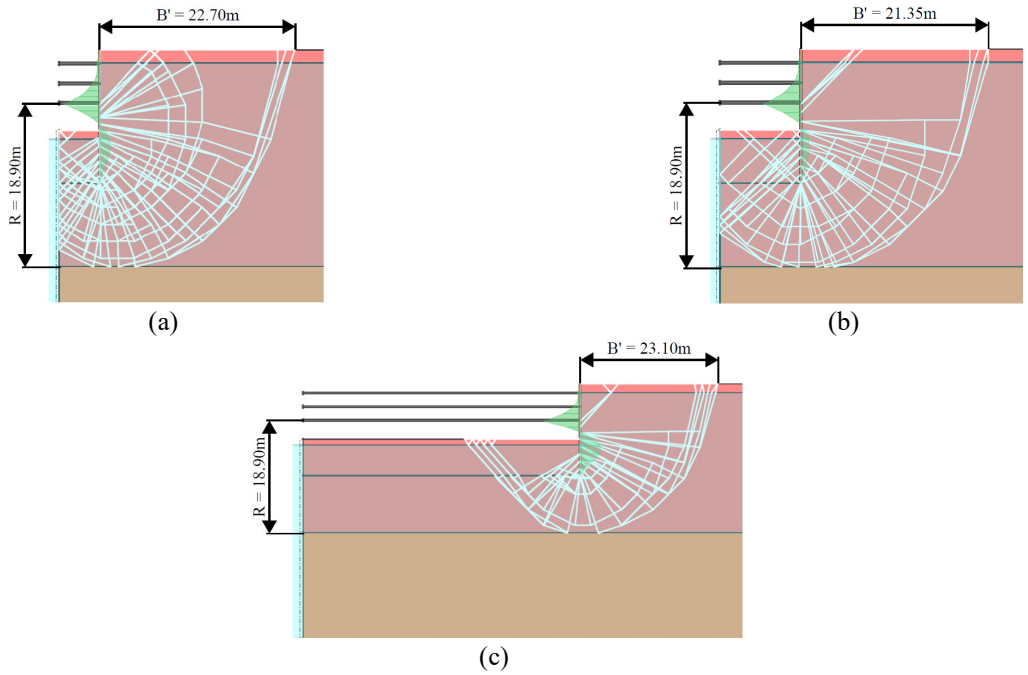

Figure 17. Basal Heave Failure Mechanisms in Case 2C: (a) $B_1/H = 0.5$ (b) $B_1/H = 1.0$ (c) $B_1/H = 5.0$

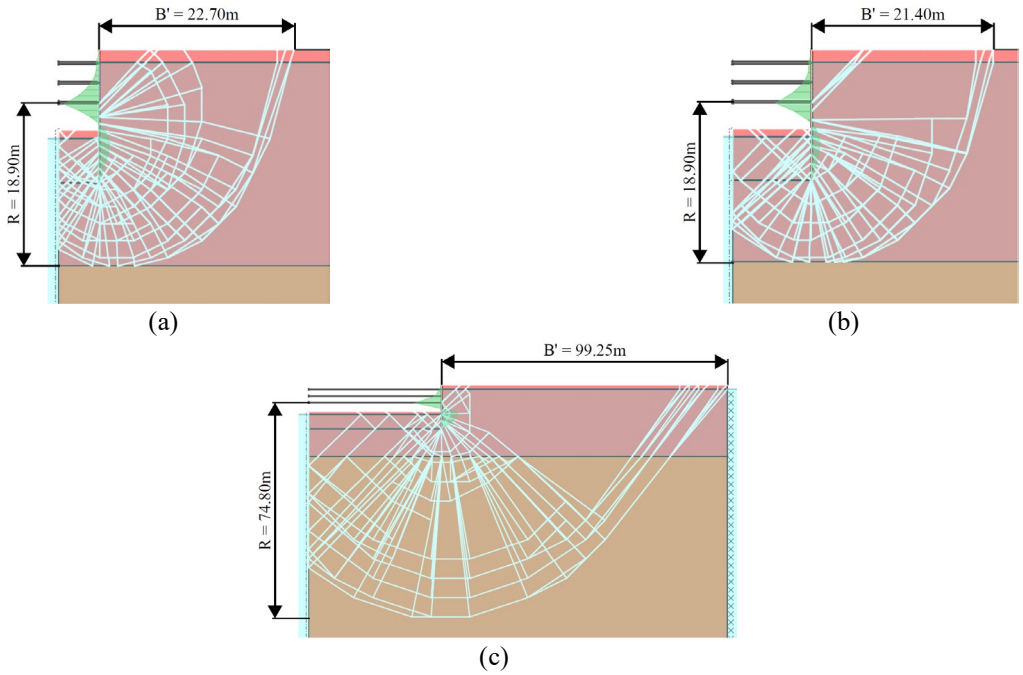

Figure 18. Basal Heave Failure Mechanisms in Case 2D: (a) $B_1/H = 0.5$ (b) $B_1/H = 1.0$ **(c)** $B_1/H = 5.0$

Discussions

Based on the conducted research, the analysis results reveal that the factor of safety (SF) values obtained using the Discontinuity Layout Optimization (DLO) method closely align with those derived from Finite Element Method (FEM) analyses in homogeneous soil models. In the study by Lim and Ou [10], two FEM-based approaches were used to evaluate basal heave stability. Method A involves reducing the undrained shear strength (Su) until the numerical model fails to converge, with the SF defined at the point of non-convergence. This approach reflects a purely numerical criterion without directly assessing physical deformation. Method B, on the other hand, evaluates SF based on observable deformation behavior. A range of strength reduction factors is applied, and the resulting displacement patterns (such as bottom heave or wall movement) are plotted. Two linear trendlines are then fitted to the displacement data, and their intersection point is used to determine the SF. This method captures the onset of failure more realistically and is considered more representative of field conditions.

When comparing the results of DLO with FEM, the values obtained from DLO are more in line with the values obtained using Method B. For example, in Case 1A, the SF obtained from DLO is 1.06, which is closer to the 1.15 reported using FEM Method B than the 1.4 from Method A. Similarly, in Case 2A, the DLO SF of 1.03 is comparable to 0.97 obtained through Method B, rather than 1.3 from Method A. This comparison shows that DLO produces a more conservative estimate, similar to the deformation-based assessment of Method B.

These findings confirm that DLO can provide reliable and relevant stability predictions under homogeneous conditions, especially when accounting for shear strength gradients. However, under layered soil conditions, differences become more apparent. DLO tends to oversimplify complex stratigraphy due to its limitations in representing abrupt changes in material properties and interface behavior.

In this more complex setting, the FEM approach offers superior modeling capabilities, particularly for the simulation of deformation, stress redistribution, and soil-structure interaction. This makes FEM more suitable for capturing field representative behavior in layered soils with heterogeneous material properties.

While DLO remains a powerful tool for identifying potential failure mechanisms in geotechnical stability problems, its application to layered soils presents several critical challenges:

- Material Discontinuities: DLO does not inherently accommodate abrupt changes in soil strength across layers, which can lead to oversimplified or unrealistic failure surface predictions.
- Interface Shear Behavior: Stress transfer and interface shear strength between layers require explicit modeling to represent localized slip or strain differentials.
- Pore Pressure Effects: The influence of groundwater and pore pressure distribution is not readily modeled within conventional DLO formulations, necessitating integration of effective stress principles.
- Mesh Representation: Limited nodal resolution at material boundaries may hinder accurate representation of interface behavior.

To address these issues, hybrid modeling approaches are recommended. For instance, integrating FEM for evaluating stress fields and pore pressure effects, while leveraging DLO for failure mechanism visualization, can provide a more robust and comprehensive analysis. Enhancements such as refined nodal connectivity at interfaces and incorporation of layer-specific constraints can also significantly improve DLO's applicability in stratified soils.

In conclusion, DLO is well-suited for preliminary assessments and conceptual design phases, particularly under homogeneous soil conditions or where computational efficiency is critical. However, for complex soil conditions involving layered profiles and non-linear shear strength gradients, FEM remains the preferred method due to its greater fidelity in capturing soil behavior. The combined use of DLO and FEM offers a synergistic framework that can enhance accuracy and insight in basal heave stability evaluations across a broad range of geotechnical scenarios.

CONCLUSIONS

This study investigated the basal heave stability of deep excavations in soft clay using the Discontinuity Layout Optimization (DLO) method and compared its performance with that of the Finite Element Method (FEM). The results demonstrate that DLO is effective and reliable in homogeneous soil conditions, where the computed factors of safety (SF) closely match those derived from FEM. This confirms DLO’s value as a rapid and insightful tool for preliminary stability assessments. Additionally, DLO provides intuitive visualizations of failure mechanisms—capturing the lateral extent (B′) and rotational depth (R) of failure zones—which aid in understanding the key geotechnical factors influencing basal heave. However, the study also revealed that DLO's accuracy diminishes in layered soil conditions, particularly where significant strength variations exist across strata. In such cases, DLO tends

to oversimplify failure mechanisms, often over-representing the influence of weaker upper layers while underestimating the stabilizing effect of stronger lower strata. This discrepancy leads to deviations in SF predictions when compared to FEM, which is better equipped to model complex deformation behavior and stress redistribution in stratified systems.

The analyses showed that in homogeneous soils, SF generally decreases as the width-to-height ratio (B_1/H), increases, in accordance with theoretical expectations. However, in layered soils, DLO may fail to capture the actual progression of failure surfaces due to limitations in how it represents material interfaces and strength heterogeneity. As a result, while DLO is a powerful tool for early-stage design, it should be supplemented by FEM for comprehensive evaluations in complex subsurface environments. Despite its strengths, this study acknowledges several limitations. The findings are based solely on numerical simulations and have not been validated against field or experimental data. Critical factors such as groundwater flow, wall embedment depth, staged construction, and time-dependent soil behavior were not included in the analyses, though they are known to significantly affect excavation stability. By refining the DLO method and combining it with complementary analytical tools, geotechnical engineers can develop more accurate, efficient, and robust excavation designs—ensuring safer and more reliable outcomes in both simple and complex soil conditions.

REFERENCES

1. Chen, R.P., Li, Z.C., Chen, Y.M., Ou, C.Y., Hu, Q., and Rao, M., Failure Investigation at a Collapsed Deep Excavation in Very Sensitive Organic Soft Clay, *Journal of Performance of Constructed Facilities*, ASCE, 29(3), 2015. https://doi.org/10.1061/(ASCE)CF.1943-5509.0000557
2. Do, T.N., Ou, C.Y., and Chen, R.P., A Study of Failure Mechanisms of Deep Excavations in Soft Clay using the Finite Element Method, *Computers and Geotechnics*, 73, 2016, pp. 153–163. https://doi.org/10.1016/j.compgeo.2015.12.009
3. Terzaghi, K., *Theoretical Soil Mechanics*, Wiley, 1943. https://doi.org/10.1002/9780470172766
4. Bjerrum, L. and Eide, O., Stability of Strutted Excavations in Clay, *Géotechnique*, 6(1), 1956, pp. 32–47. https://doi.org/10.1680/geot.1956.6.1.32
5. JSA, *Guidelines of Design and Construction of Deep Excavation, Japanese Society of Architecture*, Tokyo, Japan, 1988.
6. Huang, M., Tang, Z., and Yuan, J., Basal Stability Analysis of Braced Excavations with Embedded Walls in Undrained Clay using the Upper Bound Theorem, *Tunnelling and Underground Space Technology*, 79, 2018, pp. 231–241. https://doi.org/10.1016/j.tust.2018.05.014
7. Do, T.-N., Ou, C.Y., and Lim, A., Evaluation of Factors of Safety Against Basal Heave for Deep Excavations in Soft Clay using the Finite-Element Method, *Journal of Geotechnical and Geoenvironmental Engineering*, ASCE, 139(12), 2013, pp. 2125–2135. https://doi.org/10.1061/(ASCE)GT.1943-5606.0000940
8. Faheem, H., Cai, F., Ugai, K., and Hagiwara, T., Two-Dimensional Base Stability of Excavations in Soft Soils Using FEM, *Computers and Geotechnics*, 30(2), 2003, pp. 141–163. https://doi.org/10.1016/S0266-352X(02)00061-7
9. Goh, A.T.C., Estimating Basal-Heave Stability for Braced Excavations in Soft Clay, *Journal of Geotechnical Engineering*, ASCE, 120(8), 1994, pp. 1430–1436. https://doi.org/10.1061/(ASCE)0733-9410(1994)120:8(1430)
10. Lim, A. and Ou, C.Y., Analysis of Basal Heave Stability for Excavations in Soft Clay Using the Finite Element Method, *Proceedings of the Third International Conference of European Asian Civil Engineering Forum*, Yogyakarta, Indonesia, Vol. 2, 2011. [Online]. Available: https://www.researchgate.net/publication/276207633
11. Chen, J., Yin, J.-H., and Lee, C.F., Upper Bound Limit Analysis of Slope Stability Using Rigid Finite Elements and Nonlinear Programming, *Canadian Geotechnical Journal*, 40(4), 2003, pp. 742–752. https://doi.org/10.1139/t03-032
12. Hawksbee, S., Smith, C., and Gilbert, M., Application of Discontinuity Layout Optimization to Three-Dimensional Plasticity Problems, *Proceedings of the Royal Society A: Mathematical, Physical and Engineering Sciences*, 469(2155), 2013. https://doi.org/10.1098/rspa.2013.0009
13. Smith, C. and Gilbert, M., Application of Discontinuity Layout Optimization to Plane Plasticity Problems, *Proceedings of the Royal Society A: Mathematical, Physical and Engineering Sciences*, 463(2086), 2007, pp. 2461–2484. https://doi.org/10.1098/rspa.2006.1788
14. Gilbert, M. and Smith, C.C., Discontinuity Layout Optimization: A New Numerical Procedure for Upper Bound Limit Analysis, *The IX International Conference on Computational Plasticity*, 2007, pp. 170–173. http://www.cladu.shef.ac.uk/
15. Bishop, A.W., The Use of the Slip Circle in the Stability Analysis of Slopes, *Géotechnique*, 5(1), 1955, pp. 7–17. https://doi.org/10.1680/geot.1955.5.1.7

16. Morgenstern, N.R. and Price, V.E., The Analysis of the Stability of General Slip Surfaces, *Géotechnique*, 15(1), 1965, pp. 79–93. https://doi.org/10.1680/geot.1965.15.1.79
17. Spencer, E., A Method of Analysis of the Stability of Embankments Assuming Parallel Inter-Slice Forces, *Géotechnique*, 17(1), 1967, pp. 11–26. https://doi.org/10.1680/geot.1967.17.1.11
18. Goh, A.T.C., Zhang, F., Zhang, W., Zhang, Y., and Liu, H., A Simple Estimation Model for 3D Braced Excavation Wall Deflection, *Computers and Geotechnics*, 83, 2017, pp. 106–113. https://doi.org/10.1016/j.compgeo.2016.10.022
19. Lin, H.-D., Wang, W.-C., and Li, A.-J., Investigation of Dilatancy Angle Effects on Slope Stability Using the 3D Finite Element Method Strength Reduction Technique, *Computers and Geotechnics*, 118, 2020, Article 103295. https://doi.org/10.1016/j.compgeo.2019.103295
20. Thendar, Y., Lim, A., and Lyman, R.A., Effectiveness of Soil Improvement for Deep Excavation in Under-Consolidated Soil: A Case Study, *E3S Web of Conferences*, 429, 2023, Article 04004. https://doi.org/10.1051/e3sconf/202342904004
21. Thendar, Y. and Lim, A., Investigation into RFD System for Deep Excavation Considering Diaphragm Wall Joints, *Rock and Soil Mechanics*, 45(12), 2024, pp. 3717–3727.
22. Ukritchon, B., Whittle, A.J., and Sloan, S.W., Undrained Stability of Braced Excavations in Clay, *Journal of Geotechnical and Geoenvironmental Engineering*, ASCE, 129(8), 2003, pp. 738–755. https://doi.org/10.1061/(ASCE)1090-0241(2003)129:8(738)
23. Smith, C.C. and Tatari, A., Limit Analysis of Reinforced Embankments on Soft Soil, *Geotextiles and Geomembranes*, 44(4), 2016, pp. 504–514. https://doi.org/10.1016/j.geotexmem.2016.01.008
24. Smith, C.C. and Gilbert, M., Advances in Computational Limit State Analysis and Design, *GeoFlorida 2010*, ASCE, 2010, pp. 119–128. https://doi.org/10.1061/41095(365)8
25. Zheng, G., Zhen, J., Cheng, X., Du, Y., Yu, D., and Song, X., Basal Heave Stability Analysis of Excavations Considering the Soil Strength Increasing with Depth, *Computers and Geotechnics*, 166, 2024, Article 106026. https://doi.org/10.1016/j.compgeo.2023.106026
26. Hsieh, P.G., Ou, C.Y., and Liu, H.T., Basal Heave Analysis of Excavations with Consideration of Anisotropic Undrained Strength of Clay, *Canadian Geotechnical Journal*, 45(6), 2008, pp. 788–799. https://doi.org/10.1139/T08-006